

# Why do rough surfaces appear glossy?

Lin Qi,<sup>1,\*</sup> Mike J. Chantler,<sup>2</sup> J. Paul Siebert,<sup>3</sup> and Junyu Dong<sup>1</sup>

<sup>1</sup>Department of Computer Science, Ocean University of China, Qingdao 266100, China

<sup>2</sup>TextureLab, Department of Computer Science, Heriot-Watt University, Edinburgh EH14 4AS, UK

<sup>3</sup>Department of Computing Science, University of Glasgow, Glasgow G12 8QQ, UK

\*Corresponding author: qilin@ouc.edu.cn

Received December 6, 2013; revised March 5, 2014; accepted March 6, 2014;  
posted March 12, 2014 (Doc. ID 202353); published April 8, 2014

The majority of work on the perception of gloss has been performed using smooth surfaces (e.g., spheres). Previous studies that have employed more complex surfaces reported that increasing mesoscale roughness increases perceived gloss [Psychol. Sci. **19**, 196 (2008), J. Vis. **10**(9), 13 (2010), Curr. Biol. **22**, 1909 (2012)]. We show that the use of realistic rendering conditions is important and that, in contrast to [Psychol. Sci. **19**, 196 (2008), J. Vis. **10**(9), 13 (2010)], after a certain point increasing roughness further actually reduces glossiness. We investigate five image statistics of estimated highlights and show that for our stimuli, one in particular, which we term “percentage of highlight area,” is highly correlated with perceived gloss. We investigate a simple model that explains the unimodal, nonmonotonic relationship between mesoscale roughness and percentage highlight area. © 2014 Optical Society of America

OCIS codes: (330.0330) Vision, color, and visual optics; (330.5020) Perception psychology; (330.5510) Psychophysics.

<http://dx.doi.org/10.1364/JOSAA.31.000935>

## 1. INTRODUCTION

Despite the fact that humans are extremely adept at using the complex interactions that occur between light and surfaces for recognizing material composition and inferring surface properties, the exact mechanism of material perception is not well understood [1].

Gloss is one of the most important of these properties, and it has been studied extensively using planar surfaces and spheres [2–4]. Initially it was studied using simple lighting conditions, such as collimated light [5], point source [6,7], and white area light [8]. However, it has been shown that more complex illumination environments approximating real-world conditions can significantly affect observers’ perceptions of materials [9,10], and indeed recent work has implied that gloss perception is not stable under changes in illumination geometry [11–13].

The majority of this work was performed using spheres or other smooth 3D shapes which meant that the influence of surface geometry at the mesoscale was not investigated. However, Vangorp *et al.* found that differently shaped objects with identical reflectance functions produced differing perceptions of gloss [14]. Olkkonen and Brainard also found that this was the case when either illumination or object shape were varied [13]. However, there has been little work reported on the perception of gloss on rougher mesoscale surfaces. Exceptions include Ho *et al.* who found that increasing the RMS height (or “bumpiness”) of a surface made of randomly deposited hemispheres, increases perceived gloss [8]. Marlow *et al.* used Ho’s surfaces to investigate the effect of varied lighting conditions [15] and showed that perceived gloss is a linear function of certain perceived properties of specular reflections, while Wijntjes *et al.* found that rough (high-magnitude RMS height deviation)  $1/f^\beta$  (colored) noise surfaces can appear

glossy to observers [5]. These fractal  $1/f^\beta$  random-phase surfaces are particularly attractive from an experimenter’s view [16], because they produce very realistic looking surfaces over a wide range of perceived roughness. They are configured using two parameters: RMS height variance and power roll-off factor. The latter being directly related to fractal dimension, while Wijntjes and Pont used the former to control roughness. Surprisingly, although their surfaces were rendered using Lambert’s law, the surfaces were perceived by observers as being glossy. However, the conditions used for producing such “glossy” surfaces were relatively unusual: relatively rough surfaces were viewed fronto-planar while being illuminated with collimated light originating from directly behind the observer. They also found that perceived gloss decreases when lighting becomes oblique. Kube and Pentland propose a theory which shows that oblique illumination of fractal surfaces can be approximated by a linear function, but that for rougher surfaces illuminated frontally, second-order effects dominate [17].

Given that work on smooth surfaces has shown that the illumination environment can significantly affect perception of surfaces, we were curious to know if we could repeat [5]. That is, the perception of glossy high-RMS height Lambertian surfaces but using more natural lighting conditions. Furthermore, we wished to determine if increasing mesoscale roughness over and above that used in [8] would continue to increase glossiness.

Hence, the study in this paper has used more realistic simulation conditions to investigate the apparent gloss described above. We used a physically based reflection model and a real-world high dynamic range (HDR) illumination map coupled with relatively high multibounce path-tracing to produce more realistic images of the  $1/f^\beta$  surfaces. Furthermore, for the second experiment we gradually rotated the surfaces to

provide the observer with motion-parallax cues regarding the surface shape, as it has been suggested that the perception of gloss is reliant on the observer's ability to understand the underlying surface relief [18].

This paper has two objectives which are addressed through two experiments. The first investigates the perceived gloss of Lambertian surfaces with high-magnitude RMS height deviation as reported by Wijntjes and Pont [5] using stimuli generated with a more sophisticated rendering system and HDR illumination maps. In the second experiment we use the same surface model and a similar environment to investigate the effect of changing surface mesoscale roughness.

The rest of this paper is organized as follows. We first describe the experimental setup that is common to the two experiments; this includes the surface model and rendering techniques. Then we describe the two experiments and go on to discuss the possible reasons behind the effect that increasing surface roughness has on perceived gloss.

## 2. COMMON EXPERIMENTAL SETUP

This section describes the surface model, rendering system, and common experimental environment for experiments 1 and 2.

$1/f^\beta$  noise was chosen as the surface geometry model to generate height maps for reasons described in the introduction. Consequently, the height maps have pseudo random-phase spectra and magnitude spectra  $H(f)$  scaled exponentially by roll-off factor  $\beta$ , as defined in Eq. (1),

$$H(f) = \frac{\sigma}{N(\beta)} f^{-\beta}, \quad (1)$$

where  $\beta$  is the roll-off factor of the surface height magnitude spectrum or the inverse slope in  $\log H$ - $\log f$  space, and  $\sigma$  is the RMS height of the surface.  $N(\beta)$  is the normalizing factor. This surface model is commonly termed as  $1/f^\beta$ , which derives from a simplification of Eq. (1). Note that the parameter  $\beta$  is inversely related to perceived roughness [19]. The magnitude spectra and phase spectra of the height maps were sampled at  $512 \times 512$  pixels. The height maps were then provided as input for the rendering system.

We employed a physics-based path tracer "LuxRender" rendering system and an HDR environment map "StPeters" from Debevec's Light Probe Image Gallery [20]. Path tracing graphics can simulate a wide range of optical effects, the most important of these being more complex surface inter-reflections. The environment map was chosen based on the fact that it is superior to other maps in the gallery in terms of resolution and dynamic range. In addition, the chosen map contains several kinds of lighting, such as skylights, windows, and bulbs, which were often simulated using directional light, area light, and point light in the literature.

Two 20 in. (50.8 cm) thin film transistor (TFT) LCD monitors (NEC LCD2090UXi) with a pixel pitch of 0.255 mm (100 dpi) were used to present the stimuli (resolution  $1600 \times 1200$  pixels). A spectrophotometer (Gretag Macbeth Eye One Pro) was used to calibrate and linearize the gamma responses (1.0). The color temperature was set to 6500 K and the maximum and minimum luminance were calibrated to 120 and 0  $\text{cd/m}^2$ , respectively. Our stimulus images have a resolution of  $512 \times 512$  pixels, and thus are square with a side-length of

13.056 cm. The monitor was set at a distance of 50 cm from the observer to provide an angular resolution of approximately 17 cpd. The stimuli subtended an angle of  $14.89^\circ$  in the vertical direction and the eyes of observer were approximately in line with the center of the screen.

Observers with normal, or corrected to normal, vision participated in the experiments. All were students or University employees working in different fields, were less than 35 years of age, and of mixed gender and nationalities. Observers were asked to provide a number that represented the "gloss" strength of each surface. The numeric range and offset of the numbers were not constrained, that is "free modulus" magnitude estimation was used. No time restrictions were imposed.

## 3. EXPERIMENT 1: APPARENT GLOSS OF HIGH-RMS LAMBERTIAN SURFACES

We investigated whether Lambertian surfaces with high-magnitude RMS height deviation were perceived to be glossy when rendered with single-bounce rendering as reported in [5] compared with when using multiple-bounce rendering and a realistic HDR environment map.

### A. Stimuli

Four  $1/f^\beta$  noise surfaces with  $\beta = 2$  and RMS height  $\sigma \in \{16, 32, 64, 128\}$  (the same parameter settings with [5]) were rendered using both single-bounce and 10-bounce path tracing under three lighting conditions: frontal, oblique ( $60^\circ$  from top), and lighting using an environment map ("stpeters" from Debevec's Light Probe Image Gallery [20]). A Lambertian reflectance model was employed in all cases. The viewing direction was perpendicular to surface plane and orthographic projection was used. Twenty-four stimulus images (four levels of  $\sigma \times 2$  rendering conditions  $\times 3$  lighting conditions) were used in total (see Fig. 1).

### B. Procedure

Five observers who participated in the first experiment were shown the 24 stimulus images in a random order and were asked to estimate surface gloss and answer the question of whether each surface appeared "matte" or "glossy."

### C. Results

The estimated gloss of each surface was normalized, averaged across all observers, and is shown in Fig. 2. The results are consistent with that of Wijntjes and Pont [5] in that perceived gloss increases with increasing RMS height under frontal illumination and decreases when lighting becomes oblique [the ANOVA test for RMS height  $\sigma$  is  $F(3, 12) = 126.309$ ,  $p < 0.001$ ]. However, a relatively low level of gloss was perceived under the real-world environment lighting [the ANOVA test for lighting conditions is  $F(2, 8) = 343.268$ ,  $p < 0.001$ ]. Additionally, the inter-reflections (multiple bounces) are not significant in this task [ $F(1, 4) = 0.012$ ,  $p = 0.917$ ], which is consistent with the findings of Wijntjes and Pont (they tested up to 2 bounces).

For the "matte or glossy" judgements, surfaces of RMS height  $\sigma = 64$  and 128 under frontal lighting were judged as "glossy" by all observers regardless of the use of single or multiple-bounce rendering. The percentage of times that surface of  $\sigma = 32$  was judged as being "glossy" is 20% for single

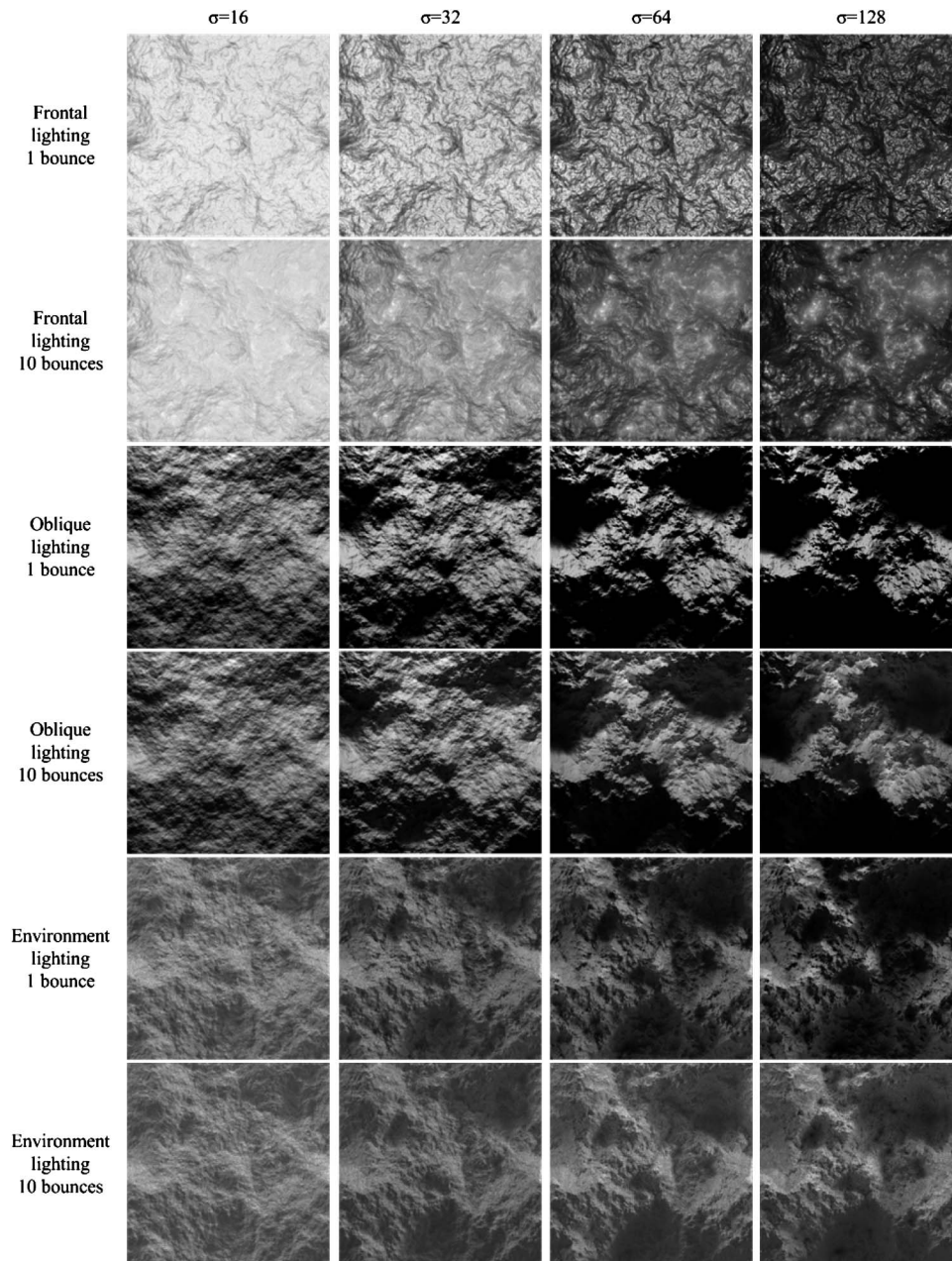


Fig. 1. Stimulus images used in experiment 1. The four columns show rendered surfaces of increasing RMS height ( $\sigma = 16, 32, 64, 128$ ). The six rows show different rendering conditions. These conditions are combinations of frontal/oblique/environment lighting and 1/10 rendering bounces.

bounce and 40% for multiple bounces under frontal lighting. For all other cases, this percentage is 0%.

Thus, we conclude that the illusory gloss of Lambertian surfaces with high-magnitude RMS height deviation was observed under a specific rendering environment, that of pure frontal illumination on rough surfaces where second-order effects dominate [17]. However, under more natural illumination conditions, that is when using an environment map, the same surfaces do not appear glossy.

#### 4. EXPERIMENT 2: DO ROUGH SURFACES APPEAR GLOSSY?

In contrast to Wijntjes and Pont [5], Ho *et al.* used a gloss (rather than a Lambertian) reflectance model [8]. They

showed that the perceived gloss of their multihemisphere surfaces, rendered using multiple-bounce reflection, initially increased with increasing RMS height and then leveled off. This variation of perceived gloss was also reported by Marlow *et al.* who used Ho's surfaces and additional lighting conditions [15].

The aim of our second experiment therefore is to investigate perceived gloss of "glossy" surfaces over a wider range of roughness and rendered under more natural conditions. In particular, we wished to see whether or not increasing roughness beyond the range that Ho *et al.* employed still provides increases in perceived gloss. We used the  $1/f^\beta$  noise surfaces as these are of more natural appearance than the multiple-half-hemisphere model. However, instead of using RMS height to vary the perceived roughness we used the roll-off factor  $\beta$ ,

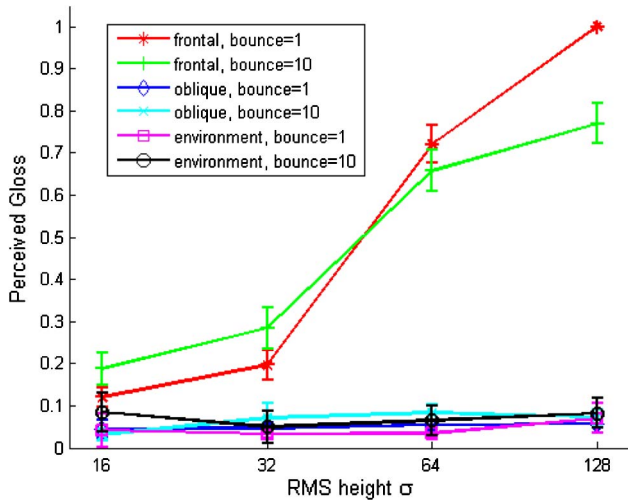


Fig. 2. Perceived gloss from experiment 1 is plotted against surface RMS height. Different markers indicate the different rendering conditions.

as this has been shown to provide a wider range of perceived roughnesses [19]. In addition, we used an HDR environment map and multiple-bounce rendering as described for experiment 1. In contrast with experiment 1, we used a physically based bidirectional reflectance distribution function (BRDF) reflection model and in order to provide observers with motion-parallax cues concerning surface shape (which has been hypothesized as being important for gloss perception) we provided animations of rotating surfaces.

### A. Stimuli

$1/f^\beta$  noise surfaces were synthesized for 14 levels of roughness with  $\beta = 1.5$  to 2.8 in steps of 0.1. The RMS height was held constant at  $\sigma = 17$ . These surfaces were rendered using the system specified previously. The environment map chosen is the same with experiment 1. The Ashikhmin-Shirley gloss BRDF model [21] was used to model the surfaces' optical property [22]. The model parameters were set to a medium gloss level ( $k_d = 0.4$ ,  $k_s = 0.6$ ,  $\alpha = 0.01$ ). The gloss level ( $\alpha$ ) used in producing stimuli was chosen to be lower than that required to exhibit distinctness of image (DOI) gloss [2,23]. The surfaces were displayed in the  $x$ - $y$  plane (the viewing direction being parallel to the  $z$  axis) and rotated through wobble angle  $w = 25^\circ$  about the vertical ( $y$ ) axis in  $1^\circ$  steps at 24 frames per second. The rendered images were linearly tone-mapped to low dynamic range to suit the capabilities of the display. Figure 3 shows the central frame images ( $w = 0^\circ$ ) of each animation stimulus, and the last two images show the surface with  $\beta = 2.8$  under  $w = 12^\circ$  and  $w = -12^\circ$ , respectively.

### B. Procedure

Nine observers participated in the experiment. Example images of glossy spheres and surface textures were shown to observers to provide them with context.

Two display monitors were used. One displayed thumbnail images ( $239 \times 239$  pixels) at wobble angle  $w = 0^\circ$  of all 14 surfaces. They were randomly positioned on the screen in a  $4 \times 4$  matrix (the last 2 squares being left blank). Clicking any thumbnail provided the full resolution ( $512 \times 512$  pixels)

rotating animation of the surface on the other monitor. Observers were able to view the full-size animations in any order and for any duration.

The task of observers was also to provide a number that represented the gloss strength of each surface. All observers finished the experiment in between 30 and 45 minutes.

### C. Results

The arithmetic means of normalized results across all nine observers are shown in Fig. 4. A one-way repeated-measures ANOVA, conducted on the normalized data, indicates that perceived gloss is significantly affected by roll-off factor  $\beta$ , with  $F(13, 104) = 37.375$ ,  $p < 0.001$ .

From Fig. 4 we can see that the perceived gloss is a non-monotonic unimodal function of roll-off factor  $\beta$ . As the surface roughness increases (and  $\beta$  reduces from  $\beta = 2.8$  to  $\beta = 2.0$ ) the perceived gloss increases in agreement with Ho *et al.* [8]. However, increasing roughness further (by reducing  $\beta$  below 2.0) results in a rapid reduction in perceived gloss.

## 5. GENERAL DISCUSSION

Two papers have reported that perceived gloss increases with increasing height-variance of bumpy or rough surfaces [5,8]. Our first experiment indicates that Lambertian surfaces of high-magnitude RMS height deviation do indeed appear glossy when rendered under similar conditions to those used by Wijntjes and Pont, but that this apparent gloss is not observed when a real-world environment map is used.

Our second experiment indicates that when a gloss BRDF model is used then our surfaces do appear glossy as expected when rendered under realistic conditions. However, in contrast with Ho *et al.*, we observe that the relationship between mesoscale roughness and perceived gloss is not monotonic. That is after a certain level of mesoscale roughness, increasing roughness further results in a decrease in perceived gloss. Similar nonmonotonic curves were also reported by Marlow *et al.* when the "primary light sources illuminated the surface obliquely" [15].

Researchers have suggested several cues observers may use to infer surface gloss and most previous work has concentrated on specular highlights and DOI gloss [2,15,23–28]. In our experiments, the microscale parameters were specifically chosen so that DOI gloss was not obvious, and thus for our surfaces it is the specular highlights that are likely to provide the most important cues.

Marlow *et al.* modeled perceived gloss as a linear function of an observer's judgement on the size, contrast, sharpness, and depth of specular reflections [15]. In contrast to Marlow *et al.*'s psychophysical approach, we chose to investigate whether the perceived gloss can be predicted using image statistics.

Specular highlights are affected by surface geometry [26,27] and are intimately related to local slope angles (as the maximum highlight normally occurs when the surface normal coincides with the half-angle of the illumination and viewing vectors). Therefore, before investigating the behavior of highlight statistics directly, we will first examine how mean slope angles are affected by changes in mesoscale roughness.

### A. Mean Slope Angle Behavior

For illustrative purposes, Fig. 5(a) shows the cross sections of three of  $1/f^\beta$  surfaces at differing mesoscale roughness

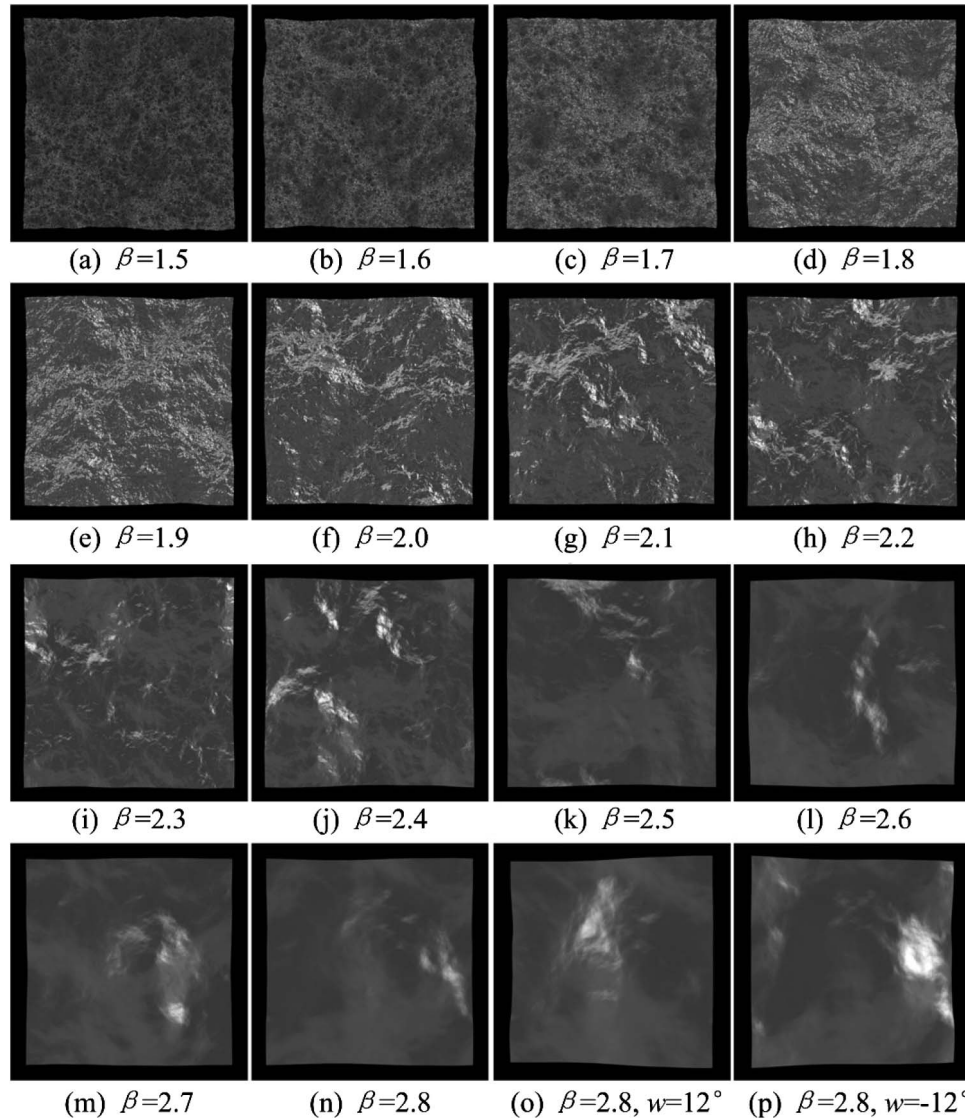


Fig. 3. (a)–(n) The central image (wobble angle  $w = 0^\circ$ ) of rendered surfaces with  $\beta$  varying from 1.5 to 2.8. (o) and (p) Surface with  $\beta = 2.8$  under wobble angle  $w = 12^\circ$  and  $w = -12^\circ$ , respectively. These images have been adjusted by a nonlinear gamma for display. Linear scaling was used for the stimuli shown to observers.

(corresponding to  $\beta = 1.6, 1.9, 2.5$ ). Note that in contrast to observer stimuli, these surfaces all have the same phase spectra so that the cross sections may be directly compared.

The absolute slope angle is the angle, ignoring sign, of the local surface normal and is obtained from the partial derivatives of the surface height maps, as  $\mathbf{n} = (-z'_x, -z'_y, 1)$ , where  $z'_x$  and  $z'_y$  are partial derivatives of the surface height maps in  $x$  and  $y$  directions, respectively. The absolute slope angle statistics are shown in Fig. 5(b) for the full range of roll-off factors ( $\beta$ ).

Figure 5(b) indicates that the mean absolute slope angle remains approximately constant over group 1 surfaces, but then increases slowly with increasing roughness over group 2, and becomes more extreme below  $\beta = 1.8$  in group 3 (with mean slope angles reaching  $65^\circ$ ). The dispersion and negative skew of the slope angles also increase with decreasing  $\beta$ .

However, while this figure gives insight into the relationship between roll-off factor ( $\beta$ ) and slope angle statistics, it

is clear that they do not correlate well at all with the nonmonotonic unimodal behavior of perceived gloss.

## B. Specular Highlights Statistics

Researchers have shown that specular highlights are important to gloss perception [13,15,24,26,27,29–31], but the particular cues that observers use to infer glossiness have not been fully established. It was found that the size, brightness (strength), contrast, sharpness, depth, orientation, and placement (spread) of specular highlights affect observers' ratings [15,24,29]. We therefore decided to analyze the behavior of the following highlight statistics: percentage area, average size, strength, number, and spread.

Unfortunately, there is no commonly agreed upon method for segmenting specular highlights and most previous investigations have undertaken manual analysis [24,26,27,29]. We have instead used a simplistic image processing technique. Since the entire stimulus set was rendered with identical reflection and illumination settings, we used a crude definition

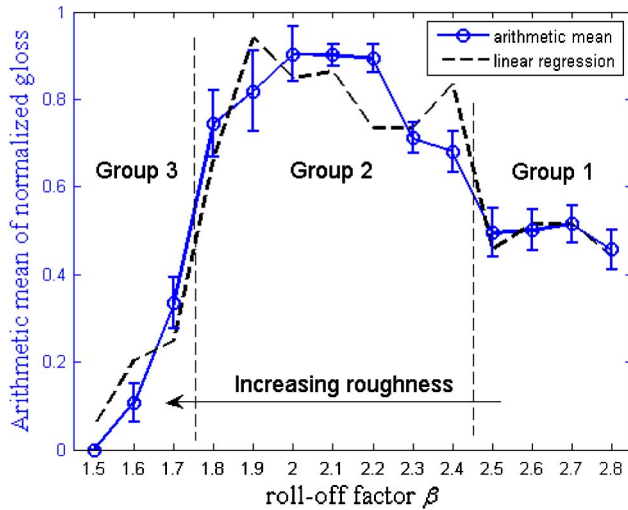


Fig. 4. Means of normalized results from nine observers are plotted using blue circles. The error bars show  $\pm$  standard errors. These data have been divided into three groups to aid later discussion. The dashed line is the regression result of perceived gloss and image processing properties reported in the general discussion.

of specular highlights based on a global intensity threshold. All pixels whose luminance values were above 50% of the global mean stimulus luminance, were assumed to be specular highlight pixels. Adjacent highlight pixels were grouped together using an eight-nearest neighborhood rule and each of the resulting “connected” components was counted as a separate “highlight area”.

The number, strength, size, spread, and percentage coverage of the highlight areas was calculated for each of the fourteen surfaces (i.e., they were calculated at each value of  $\beta$  by averaging over the 25 images rendered from each surface). The “number” refers to mean number of connected components, also averaged over the 25 images rendered from each surface. The “strength” of specular highlights refers to mean highlight pixel intensity. The number of pixels contained within each highlight was used to calculate the mean “size” of highlights. The 2D centroid of each connected component was used both to represent the location of each highlight, and to calculate their “spread” (spatial variation). The ratio of the

total number of highlight pixels to the total number of surface pixels was used to derive the average “percentage” coverage of highlight areas.

The correlation coefficients for each of the following statistics (against perceived gloss) were calculated

- spread:  $\rho = 0.12$ ,  $p = 0.68$ ;
- size:  $\rho = -0.13$ ,  $p = 0.65$ ;
- number:  $\rho = 0.59$ ,  $p < 0.05$ ;
- strength:  $\rho = 0.77$ ,  $p < 0.01$ ;
- percentage:  $\rho = 0.90$ ,  $p < 0.001$ .

We used multiple linear regression to investigate the relationship between these five image statistics and perceived gloss in a similar manner to that employed by Marlow *et al.* [15] when they investigated the relationship between gloss and perceived image cues. The results of the above investigation are plotted in Fig. 4 with statistics  $R^2 = 0.91$ ,  $F = 16.19$ ,  $p < 0.001$ .

From the above it can be seen that although the number and strength of specular highlights both exhibit significant correlations with perceived gloss, it is the percentage of highlights that shows the closest (linear) relationship, accounting for 81% of the variance in the data ( $\rho = 0.90$ ,  $p < 0.001$ ) and that this only increases to 91% when a linear combination of all five image statistics is used.

Furthermore, it can be seen from Fig. 6 that the percentage of highlight pixels clearly follows a nonmonotonic behavior that is similar to that exhibited by the perceived gloss in experiment 2 as shown in Fig. 4. Marlow *et al.* [15] reported that the perceived “coverage” of specular reflections is a dominant cue in gloss perception when surface images mainly differ in coverage. Please note that the term “coverage” used by Marlow *et al.* has a similar meaning with our term “percentage of highlight pixels.” However, our measure is calculated directly from the image, whereas Marlow *et al.* used human observers to estimate this cue.

It should be noted that we are not suggesting that this provides proof of a causal relationship but that given a set of random-phase surfaces illuminated under the same environmental conditions, it does show that the area of highlight and the perceived gloss of these surfaces are significantly related. Of course this assumes that the “highlights” are located

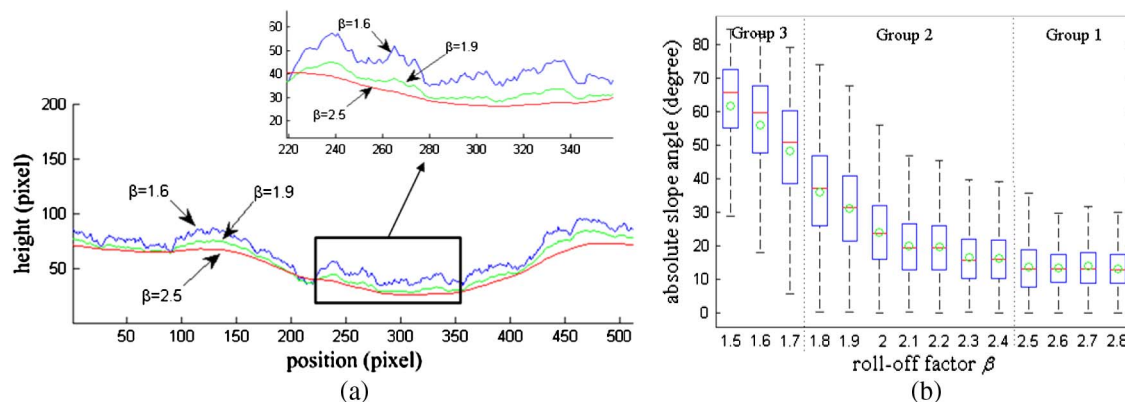


Fig. 5. (a) The cross sections of surfaces  $\beta = 1.6, 1.9, 2.5$ . The surfaces were generated using an identical random-phase spectrum for ease of comparison by the reader. Stimuli generated for observers used different phase spectra. (b) Box-plots of absolute slope angle statistics of the stimuli surfaces used in the experiment. For each surface  $\beta$ , the green circles denote the mean absolute slope angle, the central red lines denote the median, the edges of the box are the 25th and 75th percentiles, and the whiskers extend to the most extreme data points (within 1.5 times the distance between 25th and 75th percentiles).

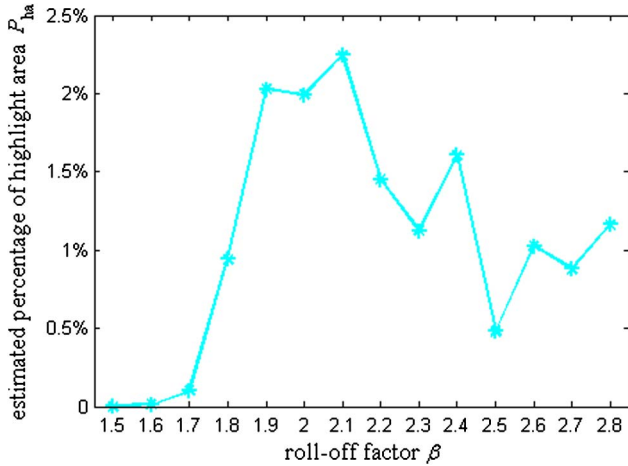


Fig. 6. Percentage of highlight area ( $P_{ha}$ ) estimated using a global threshold of 50% luminance plotted against  $\beta$ .

in the appropriate locations given the underlying surface topology, as counterexamples could easily be constructed [31].

In the next section we investigate a possible explanation for this nonmonotonic behavior.

### C. Behavior of $P_{ha}$ (Percentage of Highlight Areas)

Inspired by the microfacet model [32], we develop a simple model that offers a possible explanation of the behavior of percentage highlight area, as a function of mesoscale roughness.

Two aspects of imaging glossy surfaces are likely to significantly affect the percentage of highlight pixels occurring in the image. Highlights occur when the local surface normal coincides with, or is near to, the half-angle of the viewing and illumination vectors [Fig. 7(a)]. However, as we have used an illumination environment instead of a single punctate light source, it is the angular distribution of bright areas within the environment that is important rather than just the angle to a single light source. We can therefore model the behavior of highlights by considering the angular distributions of the

surface slope angles and the distribution of bright areas within the “St.Peters” illumination map [Fig. 7(b)]. Furthermore, as the surfaces are isotropic they have a uniform distribution over the slope tilt angle and we can ignore the effect of rotation about the  $z$  axis.

We therefore estimated the percentage highlights in a two stage process: first we integrated the environment map over tilt angle to obtain the marginal distribution of “strong” light sources as a function of slant angle, and second we combined this with the corresponding marginal distribution (over slant) of surface slope angles. Essentially, we wished to estimate the illumination distribution (as a function of slant angle) and compare this with the slope angle distribution (as a function of their half-angle).

In order to simplify estimation of the marginal distribution of strong light sources in the environment [ $P_e(\theta_i)$ ] we cropped the illumination map (incident slant angle  $\theta_i \leq 90^\circ$ ) and converted it to a binary image  $E_{ls}$  using a crude global threshold (luminance greater than 1 in its original HDR). The slant angle distribution was calculated by summing over tilt using Eq. (2) and is shown as the blue bar chart in Fig. 8(a)

$$P_e(\theta_i) = \frac{1}{N(\theta_i)} \sum_{\phi_i=0^\circ}^{360^\circ} E_{ls}(\theta_i, \phi_i), \quad (2)$$

where  $E_{ls}(\theta_i, \phi_i)$  is the binary environment map after applying the luminance threshold and  $N(\theta_i)$  is the normalization factor which is the total number of pixels in the environment map with incident slant angle  $\theta_i$ .

In the second step, the sum of products of this distribution  $P_e(\theta_i)$  and the slope angle distribution (their unnormalized correlation) were used to estimate the percentage of highlight area [ $P_{ha}^*(\beta)$ ]

$$P_{ha}^*(\beta) = \sum_{\theta_i=0^\circ}^{90^\circ} P_s(\theta_i/2; \beta) \cdot P_e(\theta_i), \quad (3)$$

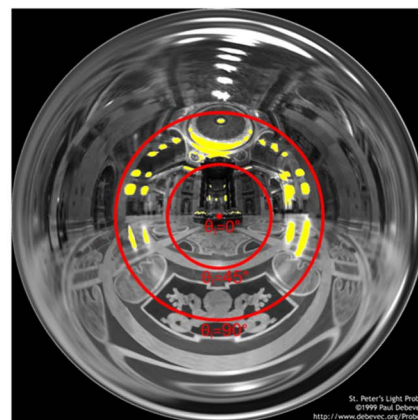
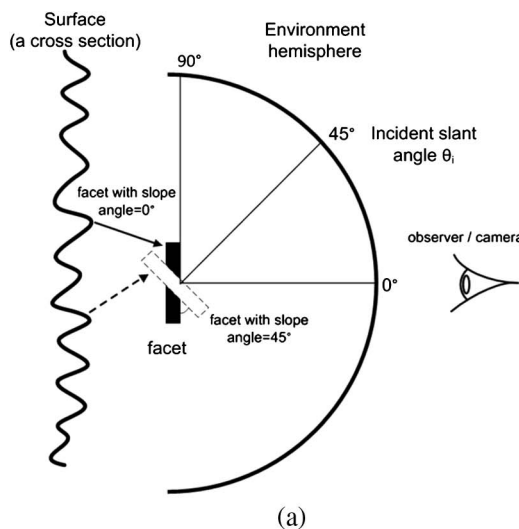


Fig. 7. (a) Schematic illustration of a facet sampling the environment illumination map. Note that the facet can only sample the illumination hemisphere up to  $90^\circ$  with a  $45^\circ$  absolute slope angle. (b) The binary image ( $E_{ls}$ ) is shown as highlighted yellow pixels which correspond to strong light sources (only the subarea  $\theta_i \leq 90^\circ$  was considered). The luminance of the environment map is also shown. The three red rings are circles of constant incident slant angle ( $\theta_i = 0^\circ, 45^\circ, 90^\circ$ ).

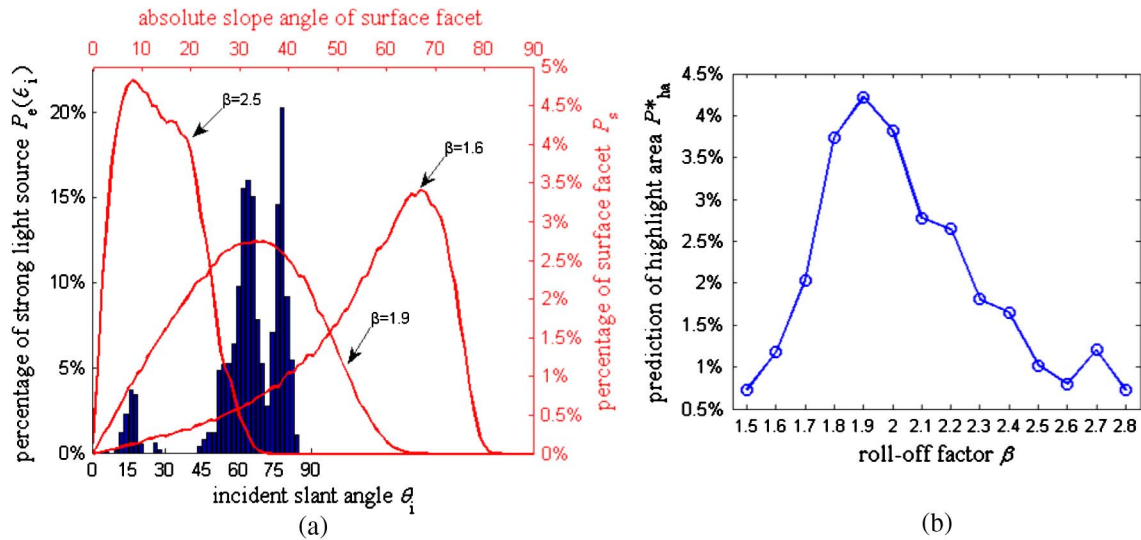


Fig. 8. (a) The marginal angular distribution of strong light sources in the illumination map is shown as a blue bar chart against incident slant angle  $\theta_i$  (bottom  $x$  axis) and the left  $y$  axis. Distributions of absolute slope angle (top  $x$  axis) for three surfaces ( $\beta = 1.6, 1.9, 2.5$ ) are plotted in red curves against the right  $y$  axis. (b) The predicted percentage of highlight areas ( $P_{ha}^*$ ) for each surface, which is calculated using Eq. (3) and the distribution of environment lighting ( $P_e$ ) and the distribution of absolute slope angle ( $P_s$ ). As can be seen from (b), the predicted highlight area value peaks at  $\beta = 1.9$  when the distribution of the half-angle of the slope facet correlates most closely with the environment distribution [see  $\beta = 1.9$  curve in (a)].

where  $P_s(\theta_i/2; \beta)$  is the marginal distribution (over tilt) of a slope angle for a surface with roll-off factor  $\beta$ .

Three illustrative plots of marginal slope distributions [ $P_s(\theta_i/2; \beta)$ ] are shown in Fig. F for three different values of  $\beta$ . Comparing these against the environment marginal distribution [ $P_e(\theta_i)$ ] shows that for  $\beta = 1.9$  there is considerable correspondence between the two angular distributions that will give rise to a high number of highlight pixels.

The predicted percentage of highlight area ( $P_{ha}^*$ ) was calculated for all values  $\beta$  used in experiment 2 and are shown in Fig. 8(b). This graph exhibits a unimodal distribution with a maximum at  $\beta = 1.9$  and which has a significant correlation ( $\rho = 0.64$ ,  $p < 0.05$ ) with the actual behavior of  $P_{ha}$  obtained using image processing (Fig. 6).

The explanation for this behavior is evident from Fig. 8(a). It shows that for a  $\beta = 1.9$  (corresponding to the peak percentage of highlights) the distribution of absolute slope angles corresponds most closely with the distribution of strong light sources in the environment. Compare this with the  $\beta = 2.5$  and  $\beta = 1.6$  slope angle distributions. Essentially, the slope angle distribution controls how many of the bright areas of the “St.Peters” illumination environment are reflected to the observer. Thus, for rougher surfaces ( $\beta < 1.8$ ), particularly in which a large number of slant slope angles exceed  $45^\circ$ , there are likely to be fewer facets capable of generating highlights. Given that the perceived gloss of these surfaces was highly correlated with the percentage of highlight pixels (experiment 2), this provides one possible explanation as to why rougher surfaces do not appear so glossy, i.e., rougher surfaces simply have higher average slope angles and hence fewer facets that are likely to reflect bright areas of the environment.

We should caution that this is clearly not an explanation for the apparent gloss observed in experiment 1. In this frontal illumination case, increasing the surface roughness by heightening surface relief clearly does not increase the number of facets that reflect the light source directly to the viewer.

Rather, the reverse is the case. The increase in apparent gloss is likely to due to the behavior of the second- and higher-order even terms which increase with RMS height, thus increasing image variance [17].

## 6. CONCLUSION

The majority of research on gloss perception has used simple surfaces such as spheres and planes. Exceptions include work by Wijnjtes and Pont [5], Ho *et al.* [8], and Marlow *et al.* [15]. Wijnjtes and Pont showed that complex Lambertian surfaces with high-magnitude RMS height deviation appear glossy when rendered under frontal lighting. In contrast, our experiments showed that such surfaces do not appear glossy when rendered using a real-world illumination environment. We conclude, therefore, that realistic illumination is a critical component to any experiment that investigates gloss on complex surfaces.

The paper by Ho *et al.* [8] that reported that perceived gloss of non-Lambertian surfaces increases with increasing “bumpiness” motivated us to ask the question, what happens if we make the surfaces even rougher? Do they still keep getting glossier? Experiment 2 showed that as one might expect, there is a limit to this behavior. Although observers reported increasing glossiness as roughness was initially increased (in agreement with [8]) after a certain point increasing roughness still further produces a very rapid reduction in perceived gloss. Thus, glossiness would appear to be a unimodal function of mesoscale roughness.

To provide further insight into this relationship, we investigated the behavior of five properties of specular highlights that have been suggested to be related to gloss perception. We used simple image processing techniques to estimate these parameters for our data set. In our experiment, perceived gloss showed weak correlations with the estimated strength and the number of specular highlights but a strong correlation with the estimated percentage of highlight area ( $P_{ha}$ ). Highlight area is a strong contender as an important

gloss cue as shown by Marlow *et al.* through experiment [15] and in this paper by using image processing statistics.

We developed a simple model of highlight area as a function of surface slope angle and illumination environment distributions. This shows that for rougher surfaces [e.g.  $\beta = 1.6$ , Fig. 8(a)] the area of highlight is dramatically reduced, as a significant proportion of the slope angles exceed  $45^\circ$  and hence are unlikely to be able to “see” the environment due to self-occlusion by the surface. Thus, it is likely that the rougher surfaces appear less glossy simply because there are fewer areas that have an unoccluded view of bright light sources in the environment.

We conclude that the correspondence of surface slope and illumination distributions is likely to play a critical role in the perception of gloss—something that jewelry shop owners have perhaps known and exploited for centuries. In future work, we intend to investigate in more detail the effect that variation of illumination distribution has on perceived gloss of complex surfaces. In addition, since the BRDF model we chose has been shown to be a poor match for wide angle gloss [33], using a wider range of BRDF models will also be part of the future work.

## REFERENCES AND NOTES

1. E. H. Adelson, “On seeing stuff: the perception of materials by humans and machines,” *Proc. SPIE* **4299**, 1–12 (2001).
2. F. Pellacini, J. A. Ferwerda, and D. P. Greenberg, “Toward a psychophysically-based light reflection model for image synthesis,” in *SIGGRAPH '00: Proceedings of the 27th Annual Conference on Computer Graphics and Interactive Techniques* (ACM/Addison-Wesley, 2000), pp. 55–64.
3. W. Fleming, R. O. Dror, and E. H. Adelson, “How do humans determine reflectance properties under unknown illumination,” in *Proceedings of CVPR Workshop on Identifying Objects Across Variations in Lighting: Psychophysics and Computation* (2001), pp. 347–368.
4. B. Xiao and D. H. Brainard, “Surface gloss and color perception of 3D objects,” *Vis. Neurosci.* **25**, 371–385 (2008).
5. M. W. A. Wijntjes and S. C. Pont, “Illusory gloss on Lambertian surfaces,” *J. Vis.* **10**(9):13, 1–12 (2010).
6. S. Nishida and M. Shinya, “Use of image-based information in judgments of surface-reflectance properties,” *J. Opt. Soc. Am. A* **15**, 2951–2965 (1998).
7. G. Wendt, F. Faul, and R. Mausfeld, “Highlight disparity contributes to the authenticity and strength of perceived glossiness,” *J. Vis.* **8**(1):14, 1–10 (2008).
8. Y. Ho, M. Landy, and L. Maloney, “Conjoint measurement of gloss and surface texture,” *Psychol. Sci.* **19**, 196–204 (2008).
9. R. W. Fleming, R. O. Dror, and E. H. Adelson, “Real-world illumination and the perception of surface reflectance properties,” *J. Vis.* **3**(5):3, 347–368 (2003).
10. R. O. Dror, A. S. Willsky, and E. H. Adelson, “Statistical characterization of real-world illumination,” *J. Vis.* **4**(9):11, 821–837 (2004).
11. K. Doerschner, H. Boyaci, and L. T. Maloney, “Estimating the glossiness transfer function induced by illumination change and testing its transitivity,” *J. Vis.* **10**(4):8, 1–9 (2010).
12. M. Olkkonen and D. H. Brainard, “Perceived glossiness and lightness under real-world illumination,” *J. Vis.* **10**(9):5, 1–19 (2010).
13. M. Olkkonen and D. H. Brainard, “Joint effects of illumination geometry and object shape in the perception of surface reflectance,” *i-Perception* **2**, 1014–1034 (2011).
14. P. Vangorp, J. Laurijssen, and P. Dutré, “The influence of shape on the perception of material reflectance,” in *SIGGRAPH '07: ACM SIGGRAPH 2007 Papers* (ACM, 2007), p. 77.
15. P. Marlow, K. Juno, and B. L. Anderson, “The perception and misperception of specular surface reflectance,” *Curr. Biol.* **22**, 1909–1913 (2012).
16. S. Padilla, “Mathematical models for perceived roughness of three-dimensional surface textures,” Ph.D. thesis (Heriot-Watt University, 2008).
17. P. Kube and A. Pentland, “On the imaging of fractal surfaces,” *IEEE Trans. Pattern Anal. Mach. Intell.* **10**, 704–707 (1988).
18. W. Ji, M. R. Pointer, R. M. Luo, and J. Dakin, “Gloss as an aspect of the measurement of appearance,” *J. Opt. Soc. Am. A* **23**, 22–33 (2006).
19. S. Padilla, O. Drbohlav, P. R. Green, A. Spence, and M. J. Chantler, “Perceived roughness of  $1/f^\beta$  noise surfaces,” *Vis. Res.* **48**, 1791–1797 (2008).
20. P. E. Debevec and J. Malik, “Recovering high dynamic range radiance maps from photographs,” in *SIGGRAPH '97: Proceedings of the 24th Annual Conference on Computer Graphics and Interactive Techniques* (ACM/Addison-Wesley, 1997), pp. 369–378.
21. M. Ashikhmin and P. Shirley, “An anisotropic phong BRDF model,” *J. Graph. Tools* **5**, 25–32 (2000).
22. We did not choose the Ward model that Ho *et al.* used in [8] because of the different rendering software we employed. These two models are similar in terms of form and rendering outcome. We believe this will not influence our stimuli and experiment.
23. J. A. Ferwerda, F. Pellacini, and D. P. Greenberg, “A psychophysically-based model of surface gloss perception,” *Proc. SPIE* **4299**, pp. 291–301 (2001).
24. J. Beck and S. Prazdny, “Highlights and the perception of glossiness,” *Atten. Percept. Psychophys.* **30**, 407–410 (1981).
25. A. Blake and H. H. Bülthoff, “Does the brain know the physics of specular reflection?” *Nature* **343**, 165–168 (1990).
26. J. Kim, P. Marlow, and B. L. Anderson, “The perception of gloss depends on highlight congruence with surface shading,” *J. Vis.* **11**(9):4, 1–19 (2011).
27. P. Marlow, J. Kim, and B. L. Anderson, “The role of brightness and orientation congruence in the perception of surface gloss,” *J. Vis.* **11**(9):16, 1–12 (2011).
28. F. B. Leloup, M. R. Pointer, P. Dutré, and P. Hanselaer, “Luminance-based specular gloss characterization,” *J. Opt. Soc. Am. A* **28**, 1322–1330 (2011).
29. J. Berzhanskaya, G. Swaminathan, J. Beck, and E. Mingolla, “Remote effects of highlights on gloss perception,” *Perception* **34**, 565–575 (2005).
30. J. B. Phillips, J. A. Ferwerda, and A. Nunziata, “Gloss discrimination and eye movements,” *Proc. SPIE* **7527**, 75270Z (2010).
31. B. L. Anderson and J. Kim, “Image statistics do not explain the perception of gloss and lightness,” *J. Vis.* **9**(11):10, 1–17 (2009).
32. M. Oren and S. Nayar, “Generalization of the Lambertian model and implications for machine vision,” *Int. J. Comput. Vis.* **14**, 227–251 (1995).
33. J. Löw, J. Kronander, A. Ynnerman, and J. Unger, “BRDF models for accurate and efficient rendering of glossy surfaces,” *ACM Trans. Graph.* **31**, 1–14 (2012).